



## THE STRAIN RATE EFFECTS ON THE COMPRESSIVE BEHAVIOR OF COMPOSITES

**Luiz Felipe Marini Silva**

**Vitor Luiz Reis**

**Mauricio Vicente Donadon**

Instituto Tecnológico de Aeronáutica – ITA, Centro Tecnológico Aeroespacial, São José dos Campos – SP, Brazil  
lfmarini@gmail.com, vreis88@gmail.com, donadon@ita.br

**Vagner Eduardo Caetano Marques**

**Viviane Queiroz da Silva**

**Evaldo José Corat**

Instituto Nacional de Pesquisas Espaciais – INPE, Centro Tecnológico Aeroespacial, São José dos Campos – SP, Brazil  
eps.eduardo@yahoo.com.br, vivianequeiroz@etep.edu.br, corat@las.inpe.br

**Abstract.** *This paper presents an experimental investigation of the strain rate effects on the dynamic behavior of woven carbon/epoxy composite laminates. Specimens were manufactured using the Resin Transfer Molding (RTM) process. The specimens were tested under compression loads at different strain rate levels using an in-house Split Hopkinson Pressure Bar (SHPB) testing apparatus. The lamination angle was varied from 0 to 90 degrees in order to investigate its influence on the dynamic behavior of composite specimens. The preliminary results indicate that the dynamic behavior of these composites is dependent on both lamination angle and strain rate effects. The proposed testing programme provides an experimental database for the development of failure criteria for spacecraft composite structures subjected to extreme loading conditions.*

**Keywords:** *strain rate effect, Split Hopkinson Pressure Bar, woven carbon/epoxy laminate.*

### 1. INTRODUCTION

In space applications, composite materials may be subjected to high velocity impact damage induced by the collisions between the structural components and meteoritic or space debris. These collisions typically occur at very high velocities, submitting the structure to extremely high energy levels leading the materials to partial or total pulverization in the contact zone. The mechanical properties of the material are strongly dependent on the strain rate involved in the collision process.

The dynamic characterization of these materials in a wide range of strain rate it's possible using a Split Hopkinson Pressure Bar (Kolsky 1949). The test consists of shooting a small cylindrical bar known as striker against an input bar, specimen an output bar. The impact of the striker generates a deformation wave that travels on the input bar. When the wave reaches the specimen, part of it is reflected and part is transmitted to the specimen generating a deformation wave being transmitted to the output bar. By measuring these three strains it's possible to determine the stress strain state of the specimen.

Experimental studies were carried out on high strain rate behavior of composites over the years under compressive loading, especially unidirectional composites and laminated composites using unidirectional layers.

Hosur et al. (2001) studied the effect of dynamic loading on the mechanical properties of carbon epoxy laminate composites using a modified split Hopkinson pressure bar (MSHPB). Their results indicated that the dynamic compressive strength through the thickness direction of cross-ply laminates exhibited a reduction as compared with the quasi-static value.

Hosur et al. (2004) studies in off-axis high strain rate compression loading of satin weave carbon/epoxy composites also observed a considerable increase of stiffness at high strain rate, as the ultimate strength and strain. Samples loaded along off-axes angle exhibit a large nonlinear response which increases with the increase of angle up to 45°.

Naik and Kavala (2008) investigated different woven fabric composite laminates and observed that for the case of plain weave carbon/epoxy along warp and fill, even though the properties are enhanced under high strain rate loading compared with those at quasi-static loading, there is no significant effect of strain rate on compressive properties at high strain rates. Lopus Puente (2012) also investigated the strain rate sensitivity of carbon/epoxy woven composites numerically and found in their analysis that strength of the composite increases with the strain rate.

Ravikumar et al. (2013) reported their experiments on woven-fabric E-glass/epoxy composites and verified a compressive strength enhancement at high strain rate loading in comparison with quasi-static loading. According to the parameters used in their experiments, the strength is increased with increasing strain rate, but the rate of increase is decreasing.

L. F. Marini, V. L. Reis, V. E. C. Marques, V. Q. Silva, E. J. Corat and M. V. Donadon  
The strain rate effects on the compressive behavior of composites

This paper aims to study the changes in the mechanical properties at high strain rate of woven carbon fiber/epoxy resin laminates and propose improvements in failure criteria when the strain rate effect is considered. In order to do that, quasi-static and dynamic tests were carried out at different fiber orientations  $(0^\circ, 90^\circ)_{21s}$  and  $(+45^\circ, -45^\circ)_{21s}$ . Based on the experimental results a modified version of the TSAI-HILL (Jones, 1998) failure criteria, incorporating strain rate effects was proposed for the investigated material.

## 2. MATERIAL, EXPERIMENTAL PROCEDURES AND DATA REDUCTION

### 2.1 Material and test specimens

The laminates were fabricated using 42 ply woven carbon fibers using the VARTM (vacuum assisted resin transfer method) process depicted in Figure 1a. The materials used were AGP193-P Hexcel woven ply and LY 5052/Araldite epoxy. The overall dimensions of the manufactured plates were 130 mm x 90 mm x 10 mm. The curing cycle followed the resin manufacturer recommendations.

Laminate quality was assessed by C-Scan based ultrasonic technique. For the dynamic tests rectangular specimens with dimensions of 14.5 mm x 10 mm x 9 mm were cut using a water-cooled diamond saw. Finally, their ends were machined in order to ensure the parallelism tolerance of 0.05mm face to face.

### 2.2 Quasi-static experimental setup

Quasi-static tests (Figure 1b) were carried out according to the ASTM D 3039 and ASTM D 3518 standards using a IITRI test rig. The tests were performed using a MTS servo-hydraulic universal testing machine at a constant displacement rate of 0.5 mm/min, equivalent to strain rate ( $\dot{\epsilon}_{qs}$ ) of  $5 \times 10^{-4}$  s. A HBM data acquisition system was used to record the strains and load during the tests.

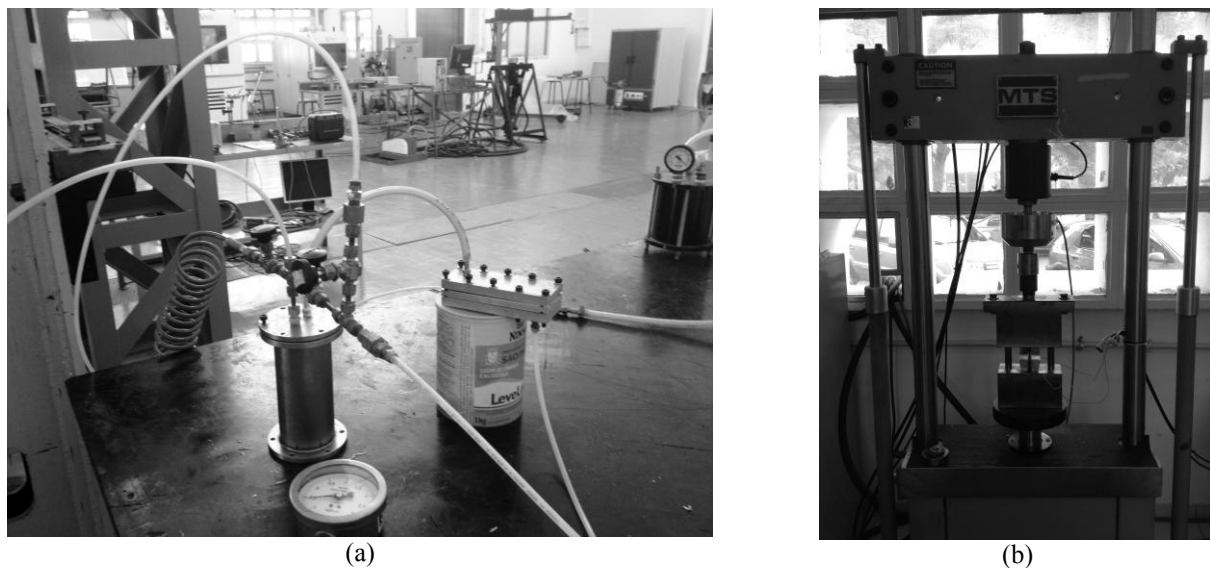


Figure 1. Material and test specimens: (a) Manufacture process; (b) Compression test.

### 2.3 Dynamic experimental setup

The characterization of composite laminate behavior in the dynamic regime was carried out using a Split Hopkinson Pressure Bar apparatus (SHPB) developed at ITA Aerospace Structures Laboratory (Fig. 2a-c). Strain rates of  $500 \text{ s}^{-1}$  was selected for the initial tests.

The SHPB is composed by a 300 mm long cylindrical steel made bar with diameter of 25.4mm, incident and transmission cylindrical bars with length of 2000 mm and diameters of 25.4mm made of steel and aluminum, respectively, both with their ends machined. Young modulus and density of the steel made striker and incident bar are  $E_{steel} = 205 \text{ GPa}$ ,  $\rho_{steel} = 7800 \text{ kg/m}^3$  whilst the aluminum made transmission bar has  $E_{al} = 70 \text{ GPa}$  and  $\rho_{al} = 2755 \text{ kg/m}^3$ . The sound wave velocity in each bar was measured using SHPB apparatus.

For strain acquisition, it was used 4 unidirectional strain gauges HBM 1-LY11-3/350, with 3 mm of gauge length. The gauges were disposed diametrically opposed in order to compensate bending. Each one of the gauges was set in a

22nd International Congress of Mechanical Engineering (COBEM 2013)  
November 3-7, 2013, Ribeirão Preto, SP, Brazil

quarter bridge arrangement. The gauges were disposed 800mm and 600 mm apart from the end of incident bar and transmission bar, respectively.

Striker velocity was measured using a couple of vibrometers in a configuration as trigger. When the striker crosses vibrometer laser light, it generates a disturbance in the signal. Measuring the distance and the time between two disturbances it is possible to measure the striker instantaneous velocity. The velocity used for the tests were between 10 and 20m/s.

The SHPB strain signals were amplified using a high speed data logger Genesis Gen7t at a sample rate of 1MHz. The signal amplification is onboard, with analog treatment and AC/DC conversion after filtering and 16bits analysis. The excitation range was  $\pm 2.5V$ . It was used a digital Butterworth filter, with cutoff frequency of 250kHz.

Before the test, the SHPB apparatus was calibrated using a free run, where both bars were kept in contact with no specimen between them. Bars transmissibility was checked comparing the transmitted signal with incident and reflected pulses. The incident and reflected pulses must be as close as possible in terms of intensity and duration, within a margin of error no more than 10%.

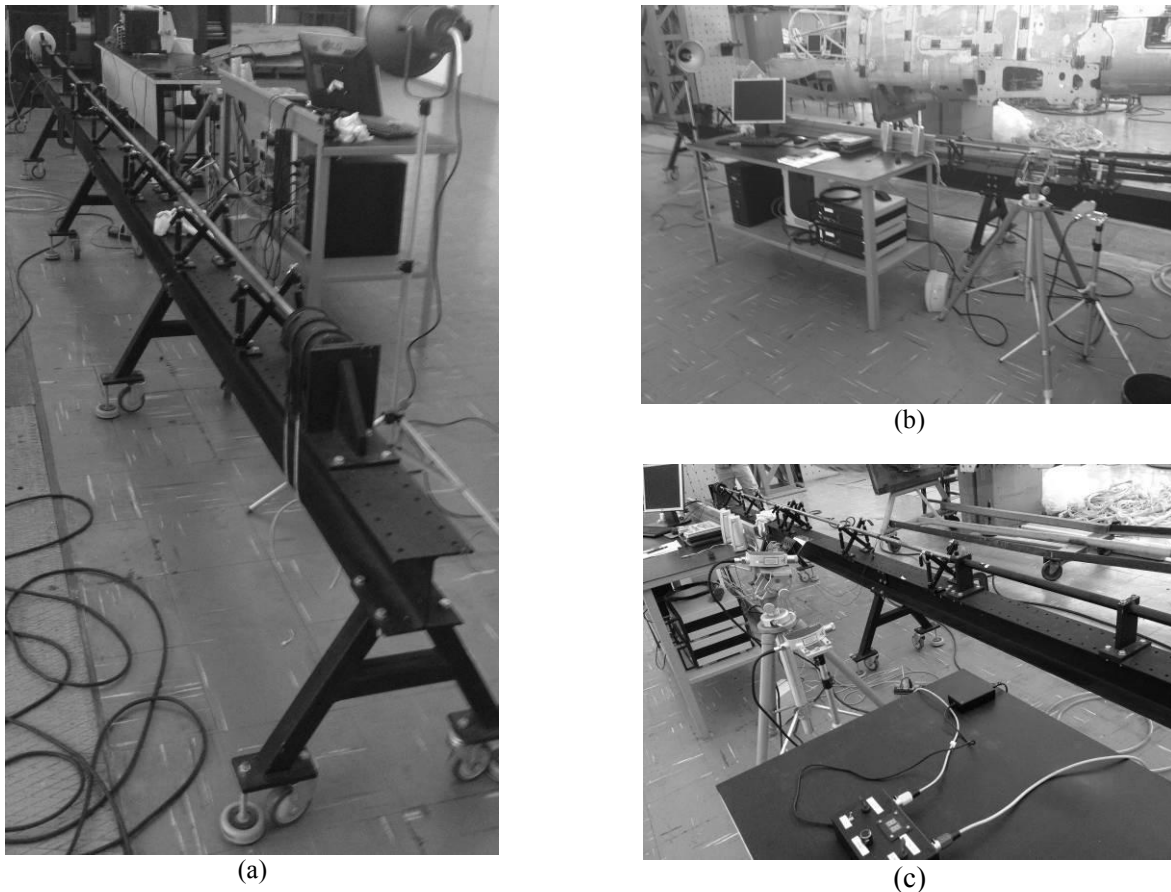


Figure 2. Experimental apparatus: (a) Split Hopkinson Pressure Bar; (b) Acquisition system; (c) Trigger.

Before the tests, the specimens were positioned between the incident and transmission bars. It was used an aluminum disc as a pulse shaper on the impacted end of incident bar. The strain signals were obtained from the data logger and preprocessed using the software HBM PERCEPTION<sup>®</sup> and post processed using an in-house developed GUI Matlab<sup>®</sup> interface. A schematic figure of the proposed SHPB test setup is depicted in Figure 3.

L. F. Marini, V. L. Reis, V. E. C. Marques, V. Q. Silva, E. J. Corat and M. V. Donadon  
The strain rate effects on the compressive behavior of composites

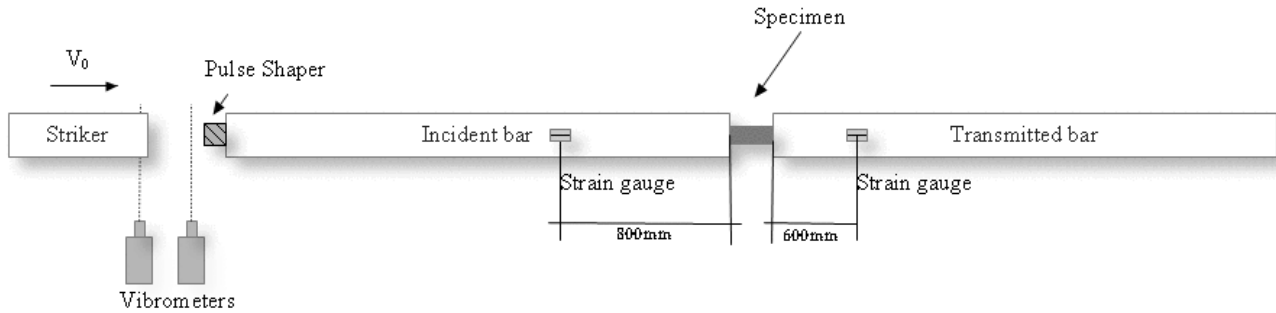


Figure 3. Split-Hopkinson pressure bar test setup.

#### 2.4 Data reduction scheme for quasi static tests

For quasi-static tests data reduction scheme was based on the ASTM D3410 (2008) and ASTM D3518 (2001). For  $0^\circ/90^\circ$  specimens the compressive stress ( $\sigma_x$ ) was calculated according to Eq. (1), where  $P$  is the applied load and  $A_s$  is the cross sectional area of the specimen.

$$\sigma_x = \frac{P}{A_s} \quad (1)$$

In the specimens of  $+45^\circ/-45^\circ$  the shear stress ( $\tau_{xy}$ ) was calculated from Eq. (2):

$$\tau_{xy} = \frac{P}{2A_s} \quad (2)$$

and the shear strain ( $\gamma_{xy}$ ) as:

$$\gamma_{xy} = \varepsilon_x - \varepsilon_y = \varepsilon_x (1 + \nu_{xy}) \quad (3)$$

where  $\varepsilon_x$  and  $\varepsilon_y$  are the strain measured in  $x$  and  $y$  directions respectively and  $\nu_{xy}$  is the Poisson ratio of the composite. The Young modulus and shear modulus were calculated using the chord method, according to Equation (4) for normal strain range of  $1000\mu\epsilon$  to  $3000\mu\epsilon$  and Equation (5) for shear strain range of  $2000\mu\epsilon$  to  $6000\mu\epsilon$ .

$$E_x = \frac{\Delta\sigma_x}{\Delta\varepsilon_x} \quad (4)$$

$$G_{xy} = \frac{\Delta\tau_{xy}}{\Delta\gamma_{xy}} \quad (5)$$

#### 2.5 Data reduction for dynamic tests

For dynamic analysis with SHPB the following equations were used (Kolsky 1949). The determination of the specimen strain is computed based on the displacement of the bar ends (incident and transmission bars). The displacements of the end of each bar is calculated as follows,

$$u_k = \int_0^t c_k \varepsilon_k(t) dt \quad k = 1, 2 \quad (6)$$

where  $c_k = \sqrt{E_k / \rho_k}$  is the velocity of the elastic wave in the bars and  $E_k$  is the Young modulus and  $\rho_k$  is the density of each bar. The deformation pulse ( $\varepsilon_k$ ) of incident bar is calculates through the difference of incident ( $\varepsilon_i$ ) and reflected ( $\varepsilon_r$ )

pulse at the instant of the impact, according to Equation (7). The compression stress was assumed to be positive throughout the paper.

$$u_1 = c_1 \int_0^t (\varepsilon_i(t) - \varepsilon_r(t)) dt \quad (7)$$

For the transmission bar, the displacement was calculated based on Equation (8),

$$u_2 = c_2 \int_0^t \varepsilon_t(t) dt \quad (8)$$

where  $(\varepsilon_t)$  is the transmitted pulse. The strain at the specimen  $(\varepsilon_s)$  with length  $L_{s0}$  is given by

$$\varepsilon_s(t) = \frac{u_1(t) - u_2(t)}{L_{s0}} = \frac{c_1}{L_{s0}} \int_0^t (\varepsilon_i(t) - \varepsilon_r(t)) dt - \frac{c_2}{L_{s0}} \int_0^t \varepsilon_t(t) dt \quad (9)$$

and the strain rate it is calculated by differentiation of Equation (9) in respect to time,

$$\dot{\varepsilon}_s(t) = \frac{c_1}{L_s} (\dot{\varepsilon}_i(t) - \dot{\varepsilon}_r(t)) - \frac{c_2}{L_s} \dot{\varepsilon}_t(t) \quad (10)$$

The forces acting at the ends of each bar in contact with the specimen are calculated as follows:

$$P_1(t) = E_1 A_1 (\varepsilon_i(t) + \varepsilon_r(t)) \quad (11)$$

where  $E_1$  and  $A_1$  are the Young modulus and cross-sectional area of incident bar, respectively.

$$P_2(t) = E_2 A_2 \varepsilon_t(t) \quad (12)$$

$E_2$  and  $A_2$  are the Young modulus and cross-sectional area of transmission bar, respectively. The specimen stress  $(\sigma_s)$  are calculated according to the Equation (13),

$$\sigma_s(t) = \frac{P_1(t) + P_2(t)}{2A_{s0}} = \left[ \frac{E_1 A_1 (\varepsilon_i + \varepsilon_r) + E_2 A_2 (\varepsilon_t)}{2A_{s0}} \right] \quad (13)$$

where  $A_{s0}$  is the initial cross-sectional area of the specimen. Figure 4(a-b) presents typical dynamic signals obtained in the experiment.

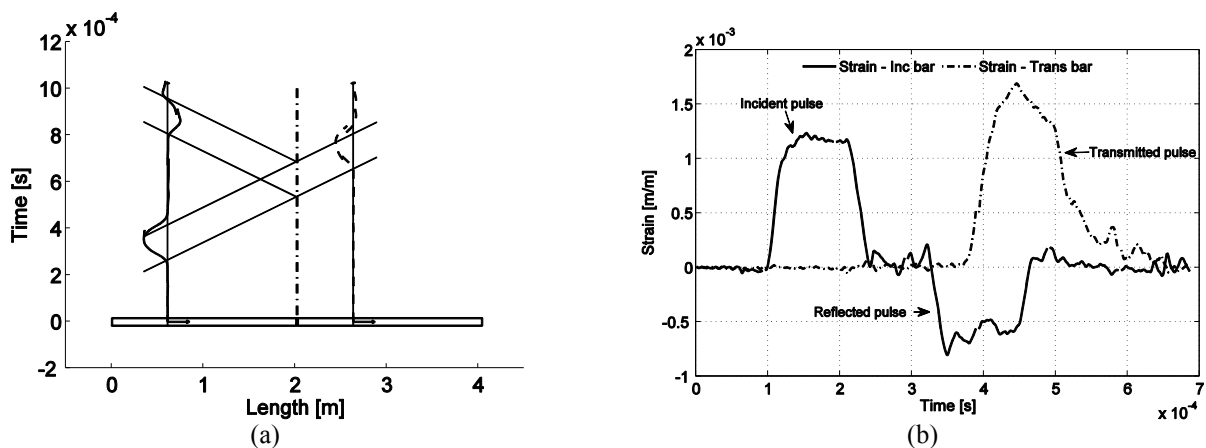


Figure 4. Dynamic test: (a) Strain pulse representation (Laplace Representation); (b) Typical recorded data from dynamic test.

In this experiment the specimen strain and specimen strain rate were obtained from a strain gauge mounted in each bar, in the positions shown in Figure 3. Since the bar strain waves  $\varepsilon_i$ ,  $\varepsilon_r$  and  $\varepsilon_t$  were measured away from the specimen

L. F. Marini, V. L. Reis, V. E. C. Marques, V. Q. Silva, E. J. Corat and M. V. Donadon  
The strain rate effects on the compressive behavior of composites

and at times before and after they have acted on the specimen. By using Fourier transformation the signals were shifted to the same starting point using Eq. (14),

$$\varepsilon_k(t) = IFFT(FFT(SG_k(t))e^{\Delta T_k \cdot \pi \cdot i}), k=i, r, t \quad (14)$$

where “*FFT*” stands for fast Fourier transform, and “*IFFT*” is the inverse of Fourier transform.  $\Delta T$  is the shifting time of the pulse based on wave speed velocity in the bar and the distance from the gauge to the bar end.

Since the separation of incident, transmitted and reflected pulses takes place, the condition to apply the classical Kolsky formulation of dynamic equilibrium is observed by monitoring the forces at each bar end. Figure 5 illustrate a typical result in terms of forces at bar ends. The results are fairly satisfactory.

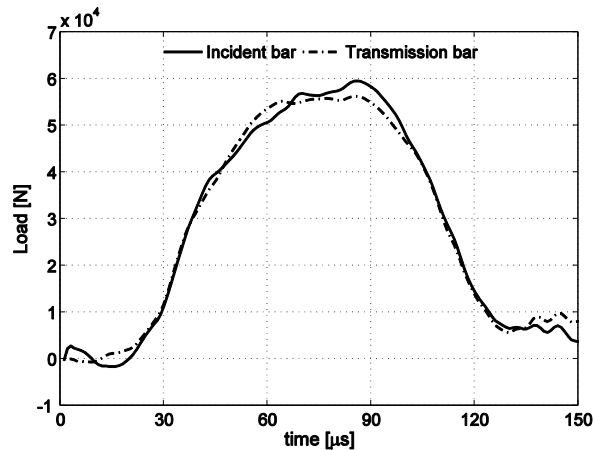


Figure 5. Forces at bar ends.

### 3. RESULTS

#### 3.1 Quasi-static results

For quasi-static analysis an amount of 6 specimens were tested (two  $(0^\circ, 90^\circ)_{21s}$  and four  $(+45^\circ, -45^\circ)_{21s}$  specimens). Figure 6(a-b) presents the stress/strain and shear stress/strain respectively and Table 1 summarizes the results obtained.

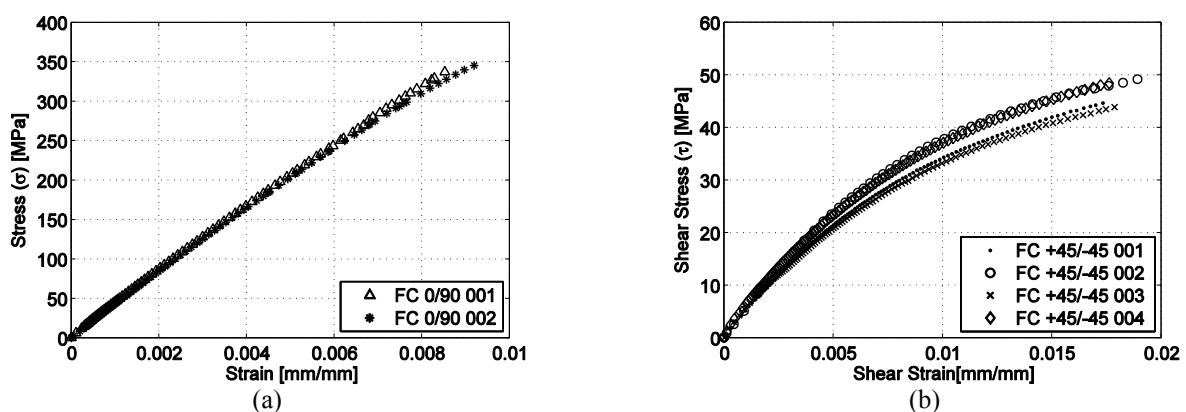


Figure 6. Quasi-static test: (a)  $(0^\circ, 90^\circ)_{21s}$  Specimens; (b)  $(+45^\circ, -45^\circ)_{21s}$  Specimens.

Table 1. Quasi-static compression properties of the composite laminate.

Specimen $(0^\circ, 90^\circ)_{21s}$	Young Modulus	Ultimate Strength
001	41.2 GPa	357 MPa
002	41.2 GPa	365 MPa
Specimen $(+45^\circ, -45^\circ)_{21s}$	Shear Modulus	Ultimate Strength
001	3.64 GPa	60.0 MPa
002	3.99 GPa	62.7 MPa

22nd International Congress of Mechanical Engineering (COBEM 2013)  
November 3-7, 2013, Ribeirão Preto, SP, Brazil

Specimen $(+45^\circ, -45^\circ)_{21s}$	Shear Modulus	Ultimate Strength
003	3.39 GPa	61.6 MPa
004	3.78 GPa	67.5 MPa

Typical failure mode of the  $(0^\circ, 90^\circ)_{21s}$  laminates occurred at fracture planes orientated between  $45^\circ$  and  $50^\circ$  in respect to the sample direction. For the  $(+45^\circ, -45^\circ)_{21s}$  specimens a typical shear band cracking orientated at  $45^\circ$  in respect to the laminate global coordinate system was observed (See Figure 7).

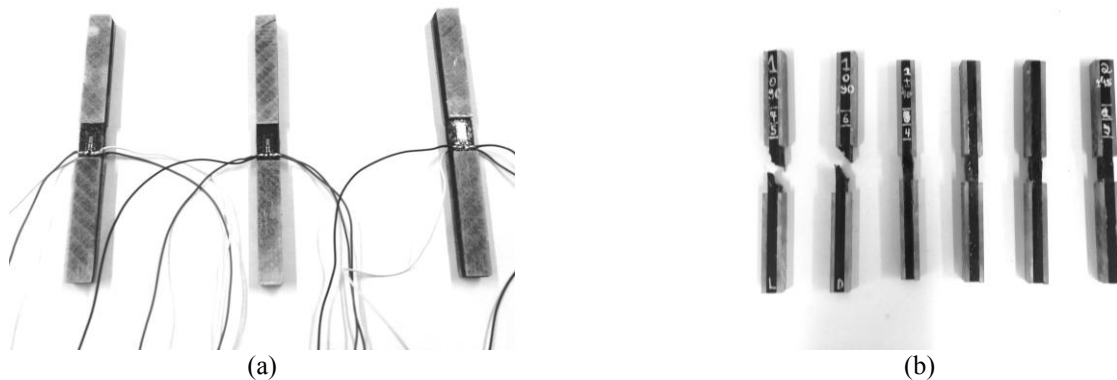


Figure 7. Quasi-static specimens: (a) Before test; (b) Mode of failure.

The average Young modulus ( $E$ ) obtained using chord method was 41.2GPa and the Shear modulus ( $G$ ) was 3.70GPa. The mean compression failure stress ( $F_{1c}$ ) measured was 361MPa and failure shear stress ( $F_{12c}$ ) was 63MPa.

### 3.2 Dynamic results

It was used the literature classical signal processing to obtain the stress, strain and strain rate along time for the SHPB apparatus. The specimens were aligned with the center of the bars as shown in Figure 8(a). The observed failure modes for the  $(0^\circ, 90^\circ)_{21s}$  laminates are depicted in Figure 8(b).

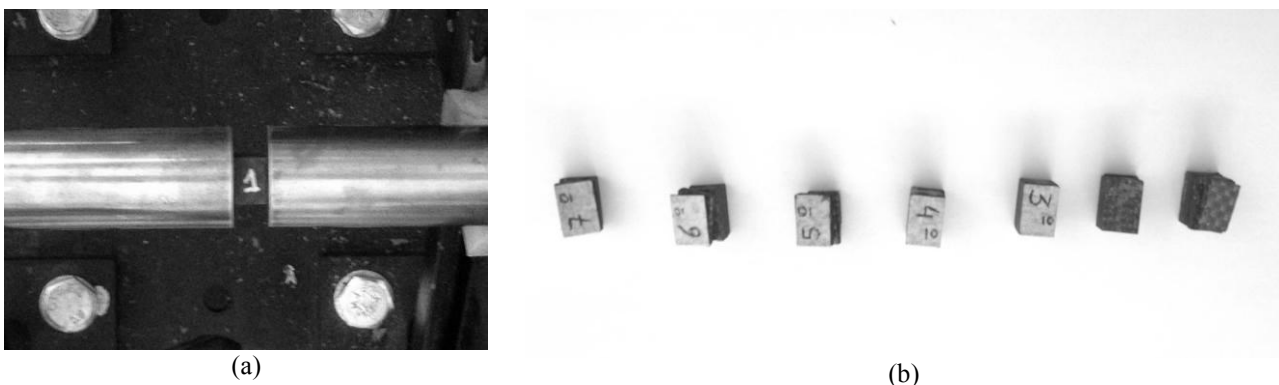


Figure 8. Specimens used in the dynamic tests: (a) Before test; (b) Mode of failure.

The signals obtained from the strain gauges were processed using an in-house GUI MATLAB® environment to obtain the stress strain curves (Figure 9a-b). No type of signal filtering was applied during the signal processing. It was generated stress, strain and strain rate curves along the time to observe the failure load (Figure 10a-b). The failure point remains well determined because it's the instant when the load starts to decrease and the strain rate also decreases.

L. F. Marini, V. L. Reis, V. E. C. Marques, V. Q. Silva, E. J. Corat and M. V. Donadon  
 The strain rate effects on the compressive behavior of composites

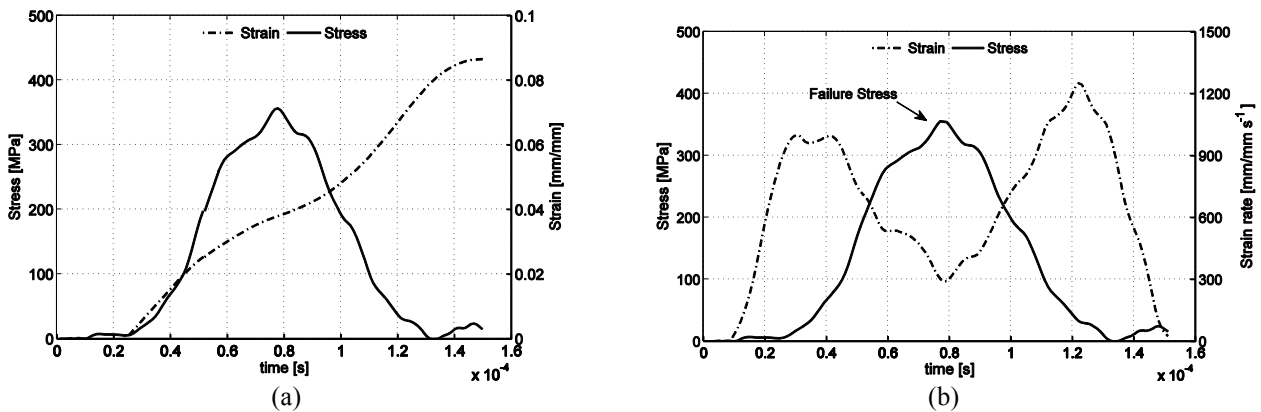


Figure 9. Typical curves along time: (a) Stress x Strain; (b) Stress x strain-rate.

To determine the strain rate, it was calculated the mean of the strain rate between the start of loading the specimen and the failure instant.

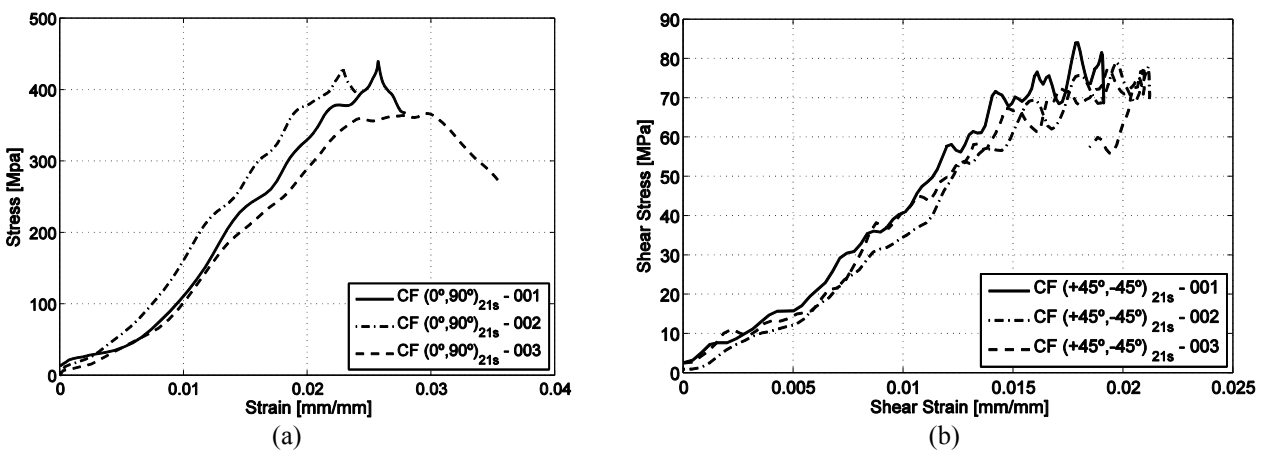


Figure 10. Dynamic stress-strain curves for: (a)  $(0^\circ,90^\circ)_{21s}$  specimens at  $500s^{-1}$  SR; (b)  $(45^\circ,-45^\circ)_{21s}$  specimens at  $500s^{-1}$ .

The results obtained from the dynamic tests for the  $(0^\circ,90^\circ)_{21s}$  and  $(45^\circ,-45^\circ)_{21s}$  laminates are listed in Tables 2 and 3, respectively.

Table 2. Dynamic results in SHPB test for  $(0^\circ,90^\circ)_{21s}$  specimens.

Specimen	Strain Rate [ $s^{-1}$ ]	Peak Stress [MPa]	Strain at peak stress [mm/mm]	Modulus [GPa]
001	497	432.0	2.27%	28.7
002	446	440.1	2.56%	21.6
003	510	360.1	2.42%	22.0
Average	-	484	2.41%	24.1

Table 3. Dynamic results in SHPB test for  $(45^\circ,-45^\circ)_{21s}$  specimens

Specimen	Strain Rate [ $s^{-1}$ ]	Peak Stress [MPa]	Strain at peak stress [mm/mm]	Modulus [GPa]
001	521	84.2	1.78%	6.7
002	535	79.3	1.96%	5.1
003	509	77.6	1.92%	4.3
Average	-	80.3	2.41%	5.3

The peak stress is related to the mode of failure of the dynamic specimen.

Figure 11. SHPB specimens  $(0^\circ,90^\circ)_{21s}$  after test.

Figures 11 and 12 shows the failure modes observed in the  $(0^\circ,90^\circ)_{21s}$  and  $(45^\circ,-45^\circ)_{21s}$  specimens, respectively. The predominant failure modes for the  $(0^\circ,90^\circ)_{21s}$  laminates include matrix cracking, interlaminar shear cracking, delamination, intralaminar shear cracking and faceting (fiber crushing). For the  $(45^\circ,-45^\circ)_{21s}$  laminates, the interlaminar and in-plane shear cracking due to fiber scissoring were the predominant failure modes. The preliminary results obtained from the dynamic tests indicate that the  $(45^\circ,-45^\circ)_{21s}$  laminates are tougher than  $(0^\circ,90^\circ)_{21s}$  laminates. For this lay-up the failure modes are resin dominated where the viscoelastic effects play an important role in the failure process. For these reasons no catastrophic failure such as multiple delamination between plies and fiber crushing were observed. Nevertheless, further tests are required to confirm this behavior.

Figure 12. SHPB specimens  $(45^\circ,-45^\circ)_{21s}$  after test.

### 3.3 Failure criterion

The difference between the quasi static and dynamic strengths of the tested material in terms of failure envelope is illustrated using the Tsai-Hill failure criterion (Jones, 1998) given as follows,

$$\left(\frac{\sigma_1}{F_{1c}}\right)^2 - \frac{\sigma_1\sigma_2}{F_{1c}^2} + \left(\frac{\sigma_2}{F_{2c}}\right)^2 + \left(\frac{\sigma_{12}}{F_{12}}\right)^2 = 1 \quad (15)$$

Assuming that the compressive strengths in directions 1 and 2 are the same for weave composite, a theoretical curve can be plotted using the results obtained from quasi-static and dynamic tests.

L. F. Marini, V. L. Reis, V. E. C. Marques, V. Q. Silva, E. J. Corat and M. V. Donadon  
The strain rate effects on the compressive behavior of composites

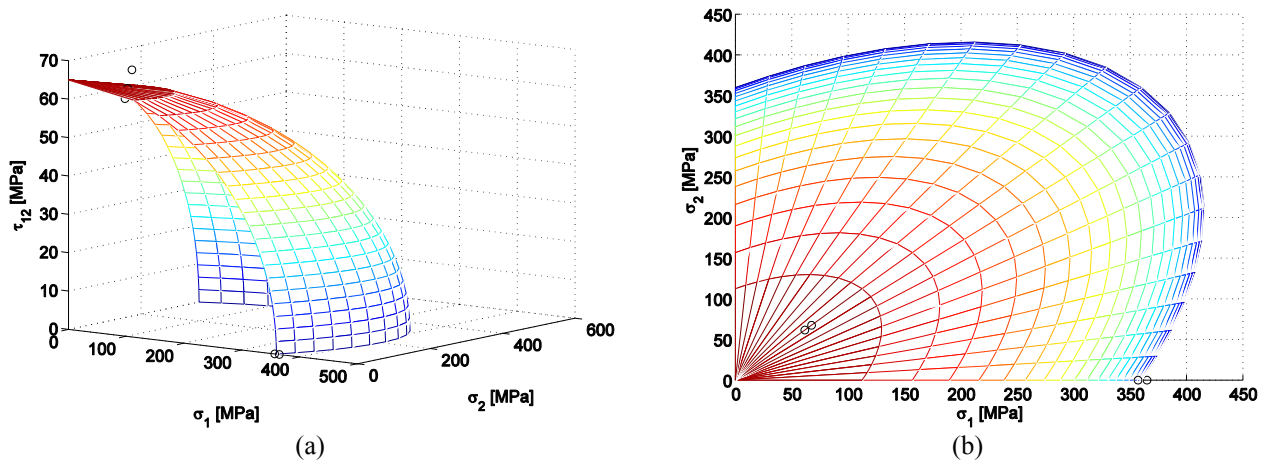


Figure 13. Tsai-hill quasi-static envelope: (a) 3D view; (b) 2D view

Since it was considered the strength in directions 1 and 2 the same, it is pertinent to plot  $\sigma_1 - \tau_{12}$  failure envelope as depicted in Figure 14.

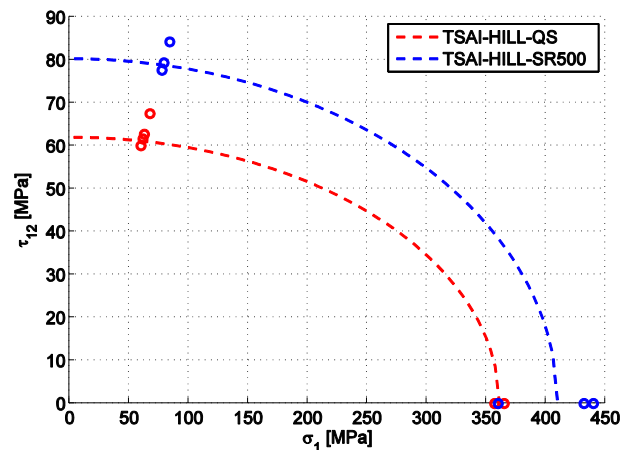


Figure 14. Failure envelope.

From figure 14 it can be observed that the failure envelope from QS loading to dynamic ( $500\text{s}^{-1}$ ) increases for higher strain rate levels. The changes in stiffness, failure strain and failure stress with strain rate are listed in Table 4.

Table 4. Quasi-static and dynamic tests comparison.

Parameter	QS	SR $500\text{s}^{-1}$	Change	QS	SR $500\text{s}^{-1}$	Change
Orientation	$(0^\circ, 90^\circ)_{21s}$			$(+45^\circ, -45^\circ)_{21s}$		
Peak Stress [MPa]	361.15	410	<b>14%</b>	63.0	80.4	<b>28%</b>
Strain at peak stress [mm/mm]	0.85%	2.42%	<b>184%</b>	1.71%	1.89%	<b>11%</b>
Elasticity Modulus [GPa]	41.2	24.1	<b>-42%</b>	3.7	5.4	<b>45%</b>

#### 4. CONCLUDING REMARKS

Investigations were carried out on 42 layer weave carbon/epoxy laminates manufactured using VARTM process under high strain rate loading. High strain rates compression tests were performed using an in-house SHPB testing apparatus.

22nd International Congress of Mechanical Engineering (COBEM 2013)  
November 3-7, 2013, Ribeirão Preto, SP, Brazil

Quasi-static and dynamic failure envelopes for compression tests were investigated and a trend of material strength enhancement in the dynamic regime was indentified. Additional tests in different strain rates will be performed in order to characterize more accurately the behavior of the material.

Further works also include the development of failure criteria and progressive failure models for composites subjected to different strain rates for spacecraft applications.

## 5. ACKNOWLEDGEMENTS

The authors would like to thank to CAPES and CNPq for the financial support and for the GSMIE of USP for know-how support.

## 6. REFERENCES

- ASTM Standard D3410 - Rev. 3, 2008. "Standard Test Method for Compressive Properties of Polymer Matrix Composite Materials with Unsupported Gage Section by Shear Loading".
- ASTM Standard D3518, 2001. "Standard Test Method for In-Plane Shear Response of Polymer Matrix Composite Materials by Tensile Test of a  $\pm 45^\circ$  Laminate".
- Hosur, M. V., Alexander, J., Vaidya, U. K., Jeelani, S., 2001. "High strain rate compression response of carbon/epoxy laminate composites". *Composite Structures*, Vol. 52, p. 405-417.
- Hosur, M. V., Alexander, J., Vaidya, U. K., Jeelani, S., Mayer, A., 2004. "Studies on the off-axis high strain rate compression loading of satin weave carbon/epoxy composites". *Composite Structures*, Vol. 63, p. 75-85.
- Jones, R. M., 1998. *Mechanics of Composite Materials*. Taylor & Francis, Philadelphia, 2<sup>nd</sup> edition.
- Koerber, H., Camanho, P. P., 2011. "High strain rate characterisation of unidirectional carbon-epoxy IM7-8552 in longitudinal compression", *Composites: Part A*, Vol. 42, p. 462-470.
- Kolsky, H., 1949. "An Investigation of the Mechanical Properties of Materials at very High Rates of Loading". *Proc Phys Soc*, Vol. B-62, p. 676-700.
- López-Puente, J., Li, S., 2012. "Analysis of strain rate sensitivity of carbon/epoxy woven composites". *International Journal of Impact Engineering*. Vol. 48, p. 54-64.
- Naik, N. K., Kavala, V. R., 2008. "High strain rate behavior of woven fabric composites under compressive loading", *Materials Science and Engineering A*, Vol. 474, p. 301-311.
- Ravikumar, G., Pothnis, J. R., Joshi, M., Akella, K., Kumar, S., Naik, N. K., 2013. "Analytical and experimental studies on mechanical behavior of composites under high strain rate compressive loading". *Materials and Design*, Vol. 44, p.246-255.
- Safa, K., Gary, G., 2010. "Displacement correction for punching at a dynamically loaded bar end". *International Journal of Impact Engineering*. Vol. 37, p. 371-384.

## 7. RESPONSIBILITY NOTICE

The author(s) is (are) the only responsible for the printed material included in this paper.